


Article

Two Unexpected Temperature-Induced Supramolecular Isomers from Multi-Topic Carboxylic Acid: Hydrogen Bonding Layer or Helix Tube

Chunyang Li ¹, Chunhong Tan ¹, Juan Zhou ^{1,2,*}, Yan-Yong Lin ^{3,*} and Xiao-Feng Wang ^{1,*} 

¹ School of Chemistry and Chemical Engineering and Hunan Key Laboratory for the Design and Application of Actinide Complexes, University of South China, Hengyang 421001, China; lcy4657857@sina.com (C.L.); tanch2014@163.com (C.T.)

² School of Mechanical Engineering, University of South China, Hengyang 421001, China

³ School of Chemistry and Chemical Engineering, Guangzhou University, Guangzhou 510006, China

* Correspondence: jzhouusc@126.com (J.Z.); linyy@gzhu.edu.cn (Y.-Y.L.); xfwang518@sina.cn (X.-F.W.)

Abstract: Under ambient conditions or 160 °C, two supramolecular isomers, namely [(H₄PTTA)(H₂O)₂ (DMF)] and [(H₄PTTA)(H₂O)₃]·Guest (**1-L** and **1-H**, H₄PTTA = *N*-phenyl-*N'*-phenyl bicyclo[2.2.2]oct-7-ene-2,3,5,6-tetracarboxydiimide tetra-carboxylic acid, Guest = DMF and H₂O), were obtained through the reaction of H₄PTTA in a mixture of H₂O and dimethylformamide. The single crystal structures reveal the temperature-dependent supramolecular isomerism derived from the torsion of semi-rigid of H₄PTTA. The **1-L** prepared at room temperature is a hydrogen bond based achiral layer, while the hydrothermal synthesized **1-H** isomer resulted in an H-bond-based chiral tubes-packed supramolecular framework.

Keywords: tetra-carboxylic acid; temperature-induced; hydrogen bonding; supramolecular isomeric; crystal structure



Citation: Li, C.; Tan, C.; Zhou, J.; Lin, Y.-Y.; Wang, X.-F. Two Unexpected Temperature-Induced Supramolecular Isomers from Multi-Topic Carboxylic Acid: Hydrogen Bonding Layer or Helix Tube. *Molecules* **2021**, *26*, 6938. <https://doi.org/10.3390/molecules26226938>

Academic Editors: Marek Chmielewski, Patryk Niedbala and Maciej Majdecki

Received: 11 September 2021
Accepted: 12 November 2021
Published: 17 November 2021

Publisher's Note: MDPI stays neutral with regard to jurisdictional claims in published maps and institutional affiliations.



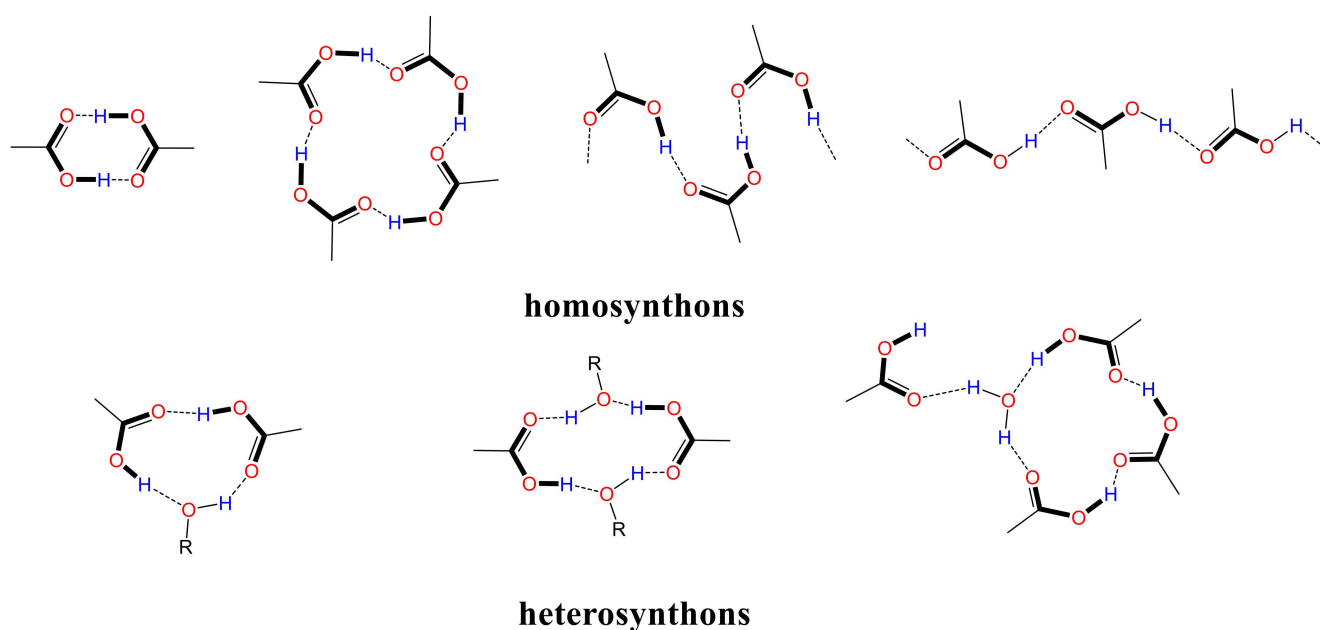
Copyright: © 2021 by the authors. Licensee MDPI, Basel, Switzerland. This article is an open access article distributed under the terms and conditions of the Creative Commons Attribution (CC BY) license (<https://creativecommons.org/licenses/by/4.0/>).

1. Introduction

Crystal engineering, traced since 1955 and accelerated in the 1980's by the independent efforts of Desiraju and other chemists, was further expanded as a fruitful research field encompassing various domains of chemistry, biology, pharmaceuticals and materials science [1–5]. In the last two decades, its development marks a shift from the analytical function of crystallography to the tuning of crystal structures, with the ultimate goal of the preparing of crystalline functional materials with promising properties [6–10]. In contrast to the hot topic branch of coordination polymers via coordination bonds, the supramolecular synthesis for the preparation of new stable solid-state materials based on non-covalent interactions, which is the original research of crystal engineering, is still relatively obscure and should be strengthened.

One of the supramolecular fundamental principles is the consideration of intermolecular interactions between molecules in the same way as the covalent bonds connecting the atoms in the molecule [11]. Therefore, it is essential to understand the interactions of direct crystal packing and sustaining in order to assemble such supramolecular solids with the aid of different specific intermolecular contacts [12–14]. Besides aromatic stacking, hydrogen bonding frequently plays an overriding dominant factor in the rational design of supramolecular assemblies. For example, the prototypal organic networks of carboxylic acid systems are usually formed through the well-known R₂²(8) eight-member carboxylic acid hydrogen bond dimers, which are considered as the concepts of supramolecular synthons [15]. Thus, the supramolecular synthon strategy has been widely applied to tailor co-crystals or supramolecular self-assemblies. Because of their strength and directionality, it is particularly useful when there are multiple functional groups capable of hydrogen bonding [16–18].

Generally, the role of hydrogen-bond synthons is now well established in supramolecular crystal engineering, and it can be categorized into two types: the homosynthons from self-complementary half units, and the heterosynthons consisting of two or more components. The dimeric, tetramer or catemeric carboxyl...carboxyl homosynthons (Scheme 1 top) within the acid molecules dominate the interaction pattern for acid crystal structures [19–21]. Although the dimeric homosynthon acts as robust, it was demonstrated that it can be expanded or disrupted by the inclusion of water or alcohols (as both donor and acceptor), in order to be changed to the heterosynthons (one or two H₂O symmetric inserting the dimmer, Scheme 1 bottom) involving -COOH and -OH, and consequently can bring up structural uncertainty [22–24].



Scheme 1. Supramolecular homosynthons (**top**) and heterosynthons (**bottom**).

The study of supramolecular isomerism is not only important in producing new materials but may also be helpful to fundamentally understanding the detail factors influencing the crystal growth process. Expected of co-crystals, the supramolecular isomerism, which comprises different structural networks derived from identical chemical compositions, is also attracting considerable investigative attentions. However, it is difficult and a great challenge to accurately predict or control the final supramolecular isomeric structures, owing to the subtle perturbation existence of thermodynamic and kinetic factors in the self-assembly process, such as different formation energy, building units' variation or intermolecular interactions. Although some temperature-induced isomeric coordination polymers have been reported [25,26], the isomerism in a hydrogen bonding network is still rare [27,28]. Herein, we report two multitopic carboxylic acid-based isomers, where the solvent water molecules of solvation are incorporated, acting as the spacer characters to tune the homosynthon to heterosynthon, while being led to form the achiral layer at ambient or chiral tube at high temperature, respectively.

2. Experimental Section

2.1. General Materials and Methods

All the reagents and solvents were commercially available and used as received without further purification. The C, H and N elemental analyses were carried out on a Vario EL elemental analyzer (Elementar, Hesse, Germany). The Raman spectrum was recorded on a Thermo Scientific DXR 3 spectrometer using KBr pellets (Waltham, MA, USA). ¹H liquid NMR spectrum was recorded with a Bruker AVANCE 300 spectrometer at

300.13 MHz (Billerica, MA, USA). Circular dichroism (CD) spectra were measured on a Jasco J-810 CD instrument (Tokyo, Japan).

N-phenyl-*N'*-phenyl bicyclo[2.2.2]oct-7-ene-2,3,5,6-tetracarboxydiimide tetracarboxylic acid (H₄PTTA) was synthesized as described in the literature [29]: a mixture of 5-Aminoisophthalic acid (1.82 g, 10.05 mmol) and bicyclo[2.2.2]oct-7-ene-2,3,5,6-tetracarboxylic acid dianhydride (1.24 g, 5 mmol) in *N,N'*-Dimethylformamide (DMF, 20 mL) was refluxed for 12 h and then cooled down to room temperature. The yellow solution was poured into 500 mL deionized water and the pH was adjusted to 2 (with 5 M HCl) to form a white suspension. White powder was filtrated, washed twice with water and dried under vacuum at 50 °C to remove the solvent water. Raman (KBr) for H₄PTTA: 3086 (m), 2960 (m), 1782 (m), 1609 (s), 1448 (w), 1391 (m), 1306 (w), 1238 (w), 1179 (m), 1089 (m), 1056 (w), 1003 (s), 940 (w), 837 (w), 799 (w), 735 (w), 699 (m), 634 (m), 588 (w), 382 (w), 216 (s), 112 (s) cm⁻¹. ¹H NMR (300 MHz, DMSO) δ (ppm): 8.48(t, J = 14, 2H, ph), 7.99 (d, J = 14.6, 4H, ph), 6.44~6.41 (m, 2H, -CH=), 3.58 (s, 2H, -CH), 3.50 (s, 4H, -CH). IR (KBr) for H₄PTTA: 3460 (s, b), 1719 (s), 1609 (w), 1459 (m), 1383 (s), 1308 (w), 1274 (m), 1190 (s), 1118 (w), 1083 (w), 1048 (w), 948 (w), 793 (m), 758 (m), 682 (m), 622 (w), 527 (w), 497 (w) and 442 (w) cm⁻¹.

2.1.1. Preparation of [(H₄PTTA)(H₂O)₂](DMF)] (1-L)

To a solution of H₄PTTA (0.162 g, 0.3 mmol) in DMF (5 mL) was added deionized water (100 mL), and then the pH value was adjusted to 2 using 2M HCl dropwise under constant stirring for 30 min. After filtered white precipitation, the clear filtrate was placed under ambient conditions; the colorless block-like crystals were isolated after slow evaporation of the solution in air for several weeks.

2.1.2. Preparation of [(H₄PTTA)(H₂O)₃]·Guest (1-H)

H₄PTTA (0.108 g, 0.2 mmol) was dissolved in a mixture of DMF (15 mL) and deionized water (5 mL) with constant stirring for 30 min. The clear solution was heated at 160 °C for 72 h under autogeneous pressure in a 25 mL sealed Teflon-lined stainless-steel vessel. After autoclave cooling to room temperature at a rate of 5 °C·h⁻¹, colorless block crystals were isolated.

2.1.3. X-ray Crystallographic Analysis

Single crystal data were collected on an Oxford CrysAlis CCD area detector diffractometer with graphite-monochromated Cu-Kα radiation (λ = 1.54184 Å) at 295(2) K. The structures were solved by direct methods and the subsequent difference Fourier synthesis was done using the SHELX-TL software suite [30]. Non-hydrogen atoms of the frameworks were refined anisotropically with hydrogen atoms generated as spheres riding the coordinates of their parent atoms. The solvent molecules in 1-H were highly disordered and were impossible to refine using conventional discrete-atom models; thus, the contribution of solvent electron density was removed by the SQUEEZE routine in PLATON [31]. The crystallographic data and structure determination parameters are given in Table 1, and selected bond lengths and angles in Table 2.

CCDC No. 2118337 and 2118346 contain the supplementary crystallographic data for the structures in this paper. These data can be obtained free of charge from the Cambridge Crystallographic Data Centre, CCDC, 12 Union Road, Cambridge CB2 1EZ, UK (Fax: +44-1223-336-033; or E-Mail: deposit@ccdc.cam.ac.uk, www.ccdc.cam.ac.uk, accessed on 11 September 2021).

Table 1. The Crystallographic data for **1-L** and **1-H** ^a.

	1-L	1-H
Empirical formula	C ₃₁ H ₂₉ N ₃ O ₁₅	C ₂₈ H ₂₄ N ₂ O ₁₅
Formula weight	683.59	628.49
Temperature	293(2)	296(2)
Crystal system	Triclinic	Tetragonal
Space group	<i>P</i> -1	<i>P</i> 4 ₃ 22
Unit cell dimensions		
a (Å)	7.0188(2)	11.0795(2)
b (Å)	13.4051(7)	11.0795(2)
c (Å)	17.4948(8)	35.0924(9)
α/°	101.590(4)	90
β/°	98.090(3)	90
γ/°	94.526(3)	90
Volume/Å ³	1586.66(12)	4307.78(19)
Z	2	4
D _{calc.} /g·cm ⁻³	1.431	0.969
μ(MoKα)/mm ⁻¹	0.994	0.080
F(000)	712	1304
R _{int}	0.019	0.080
Reflections collected	9130	9844
Observed reflections [<i>I</i> > 2σ(<i>I</i>)]	4322	4446
Flack parameter	0	0.1(16)
Goodness-of-fit on F ²	1.05	1.12
R ₁ [<i>I</i> > 2σ(<i>I</i>)]	0.0457	0.0461
wR ₂ (all data)	0.1226	0.1365
Largest diff. peak and hole/e.Å ⁻³	1.08 and −0.47	0.29 and −0.28

$$^a R_1 = \sum |F_o| - |F_c| / \sum |F_o| \cdot wR_2 = [\sum w(F_o^2 - F_c^2)^2 / \sum w(F_o^2)^2]^{1/2}.$$

Table 2. Hydrogen bond parameters (Å, °) in the crystal structures of **1-L** and **1-H**.

1-L				
D-H...A	d(D-H)	d(H...A)	d(D...A)	<(DHA)
O1W-H1WA...O6 #1	1.010	1.730	2.735(3)	172
O1W-H1WB...O2W	1.060	1.640	2.684(3)	167
O3-H3...O4 #2	0.970	1.640	2.607(2)	178
O2W-H2WA...O13 #3	0.890	1.880	2.768(4)	171
O2W-H2WB...O13 #4	1.000	1.820	2.819(3)	173
O5-H5...O9 #5	0.940	1.710	2.628(2)	166
O10-H10...O1W #3	0.990	1.520	2.506(3)	173
O12-H12...O11 #6	1.050	1.560	2.593(2)	168
C6-H6...O8 #1	0.980	2.580	3.410(3)	143
C8-H8...O2 #7	0.930	2.540	3.309(3)	140
C31-H31B...O2 #7	0.960	2.510	3.366(4)	148
Symmetry codes: #1 = 2 - x, 2 - y, 1 - z; #2 = 1 - x, 2 - y, - z; #3 = - x, 1 - y, 1 - z; #4 = 1 + x, y, 1 + z; #5 = 2 + x, 1 + y, z; #6 = 1 - x, - y, 1 - z; #7 = - 1 + x, y, z.				
1-H				
D-H...A	d(D-H)	d(H...A)	d(D...A)	<(DHA)
O2W-H2WA...O1 #1	0.85	2.11	2.883(2)	150
O2W-H2WB...O4 #2	0.85	1.95	2.784(3)	167
O2-H2A...O2 #3	0.86	1.6	2.440(2)	164
O3-H3...O2W	0.81	1.94	2.713(3)	160
O1W-H1WA...O2W	0.85	2.03	2.884(3)	177
C3-H3A...O3 #4	0.98	2.46	3.076(6)	121
Symmetry codes: #1 = x, 2 - y, 1/2 - z; #2 = - 1 + y, 1 + x, 1/4 - z; #3 = x, 1 - y, 1/2 - z; #4 = - 1 + y, x, 1/4 - z.				

3. Results and Discussion

3.1. Structural Description of $[(H_4PTTA)(H_2O)_2(DMF)]$ (**1-L**)

Solvates of H_4PTTA from a DMF/water mixture solution under an ambient condition, namely **1-L**, gave high-quality crystals. As depicted in Figure 1, single crystal X-ray diffraction (SCXRD) shows that **1-L** crystallizes in triclinic system with centrosymmetric space group P-1. An asymmetric unit contains one crystallographically tetra-carboxylic acid H_4PTTA molecule, two water molecules and one DMF molecule. The bicyclo[2.2.2]oct-2-ene unit in the H_4PTTA is a boat-like conformation with the dihedral angle between pyrrol rings of 122.27° . The torsion angles between pyrrol and phenyl rings of isophthalic acid are 58.35° and 51.84° , respectively. The two phenyl rings from isophthalic acid moieties rings are non-coplanar and form dihedral angles of 23.72° , while both planes defined by the $-COOH$ group are almost coplanar with the dihedral angle of 3.60° . Within the H_4TPPA molecule, there are two types of strong hydrogen bond motifs: $R_2^2(8)$ eight-member dimeric carboxylic homosynthon and one water inserted ten-member heterosynthon (Figure 1a). Each H_4TPPA features two homosynthons and two heterosynthons. Two H_4PTTAs combined with two isophthalic acid moieties from adjacent H_4PTTA to form two different apertures: dumbbell and oval, respectively (Figure 1d,e), while one was fulfilled with lattice H_2O and DMF molecules. Besides these conventional hydrogen bonds, there are two unconventional $C-H\cdots O$ hydrogen bonds between the $-CH_3$ from the DMF and O atoms from two kinds of groups (carboxyl and aldehyde group with the $C-H\cdots O$ distances of 3.440 \AA and 3.366 \AA , respectively), which are not only a steric effect but also play a significant role in the formation of supramolecular assembly. These acid moieties are linked via two kinds of H-bond synthons to form a 2-D herringbone pattern layer along $[100]$ direction (Figure 2a). Furthermore, the adjacent 2-D layer arrays stack in an off-set mode along the (100) direction, holding via weak $C-H\cdots O$ H-bonds between bicyclo[2.2.2]oct-2-ene unit and O atom from lattice water or pyrrolidine-2,5-dione segment to form a 3-D supramolecular structure. This suggests weak $C-H\cdots O$ interaction forces consolidate the whole supramolecular system.

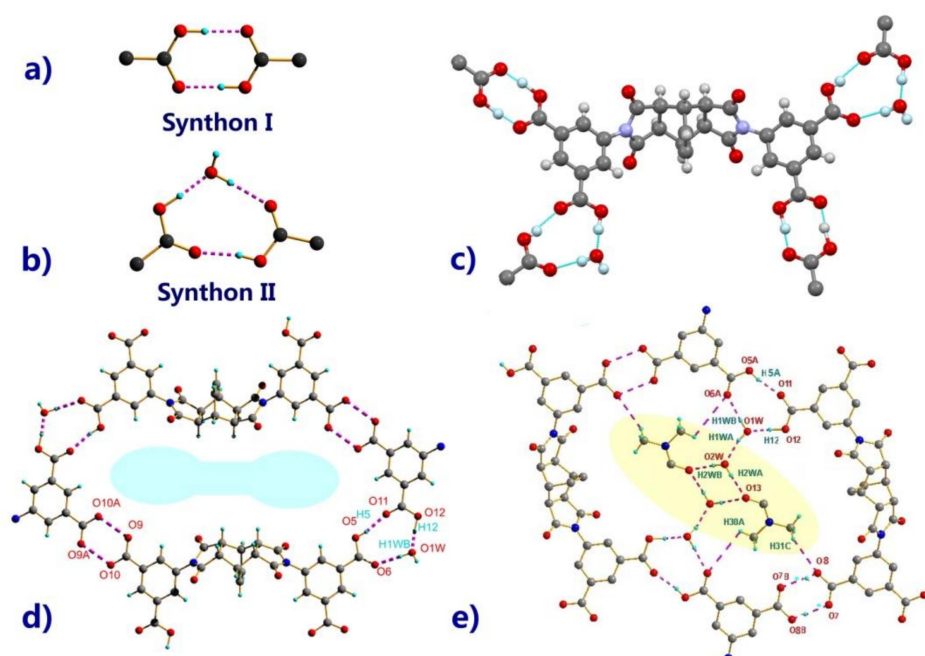


Figure 1. The homosynthon and heterosynthon (a,b); the H-bonds environment of one H_4PTTA (c); two types of apertures: void (d) and fulfilled by lattice H_2O and DMF (e) in **1-L**.

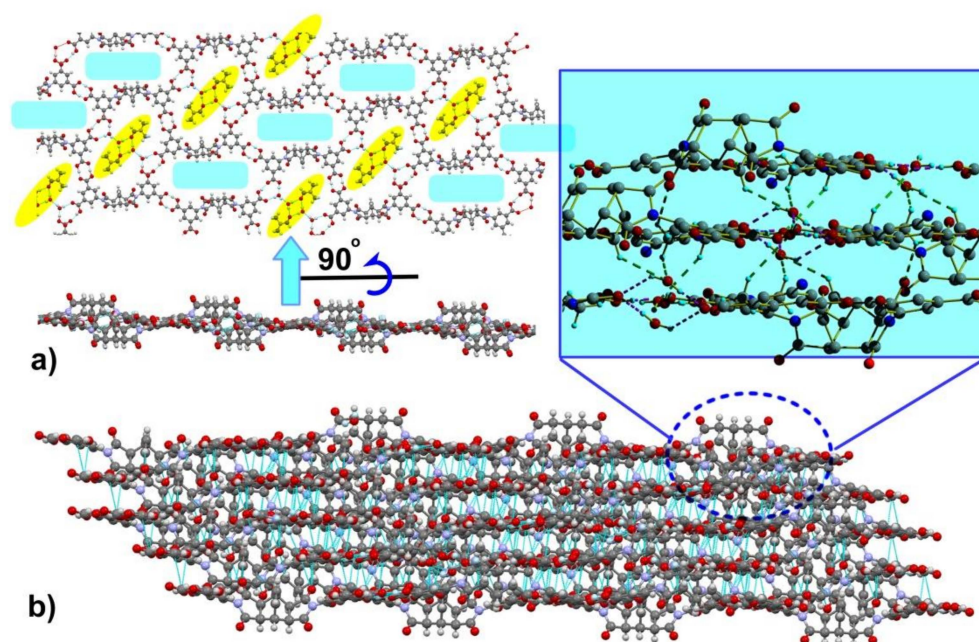


Figure 2. The top and side views of the two-dimensional hydrogen bond layer (a); the off-set packing of the two-dimensional hydrogen bonded sheets and interactions between adjacent layers (b) in **1-L**.

3.2. Structural Description of $[(H_4PTTA)(H_2O)_3] \cdot \text{Guest} (\mathbf{1-H})$

Colorless block crystals can be obtained from DMF/water mixed solution at high temperature (160 °C), namely **1-H** with guest molecules of DMF and H₂O. SCXRD shows that **1-H** crystallizes in a tetragonal system with chiral space group $P4_322$. The asymmetric unit contains a half of a crystallographically tetra-carboxylic acid H₄PPTA molecule and one and a half water molecules. Similar to **1-L**, the bicyclo[2.2.2]oct-2-ene unit center of the H₄PPTA molecule also adopted symmetric boat-like conformation, with a somewhat different dihedral angle between pyrrol rings of 123.68°. Within the H₄TPPA molecule, the angles between phenyl rings of isophthalic acid segments and pyrrol rings are both 65.70°. It is worth noting that the angle of the phenyl ring plane of the isophthalic acid is obviously different from that in **1-L**, which is 39.25° larger than 23.72°. The two planes defined by the -COOH groups of the isophthalic acid segments are also non-coplanar with a dihedral angle of 4.93 or 16.59°, respectively. Each H₄TPPA molecule holds eight hydrogen bonds featuring two kinds of H-bond motifs: three water inserted 11-member heterosynthons, and one water inserted 7-member heterosynthon (Figure 3a,b, respectively). Notably, in the 11-member heterosynthon, the H₂O molecules feature different roles: one H₂O acting as two H-bond donors (O1W-H···O, 2.884 Å), while another one acts as two H-bonds donors and two acceptors (O2W-H···O, 2.713, 2.784, 2.883 and 2.884 Å). Meanwhile, carboxylic groups act as H-bond donors and acceptors with a chelate model. The H₄TPPA molecules are connected by these hydrogen bonds of two carboxylic acid groups: one is mode IV (Figure 3b), while another one is mode III (Figure 3a), in which the water molecule holds four hydrogen bonds as a bridge. In addition, the semi-rigid H₄TPPA molecule has a C–N bond which can rotate with a certain angle, which hydrogen bonds combine together to construct a one-dimensional (1-D) infinite right-hand helix chain along the *b*-axis (see Figure 4a). Further, the adjacent 1-D chains array stack in an off-set mode along the *c*-axis to form right-hand helix tubes with a diameter of 18.22 Å, through interlayer mode III and IV H-bond heterosynthons. The extended three-dimensional (3-D) homo-chiral supramolecular network with rhombic hydrophilic channels (fulfilled with guest molecules of DMF and H₂O) is eventually constructed via interlayer hydrogen bonds involving the lattice water and resting carboxyl of H₄TPPA tetra-acid (see Figure 4d).

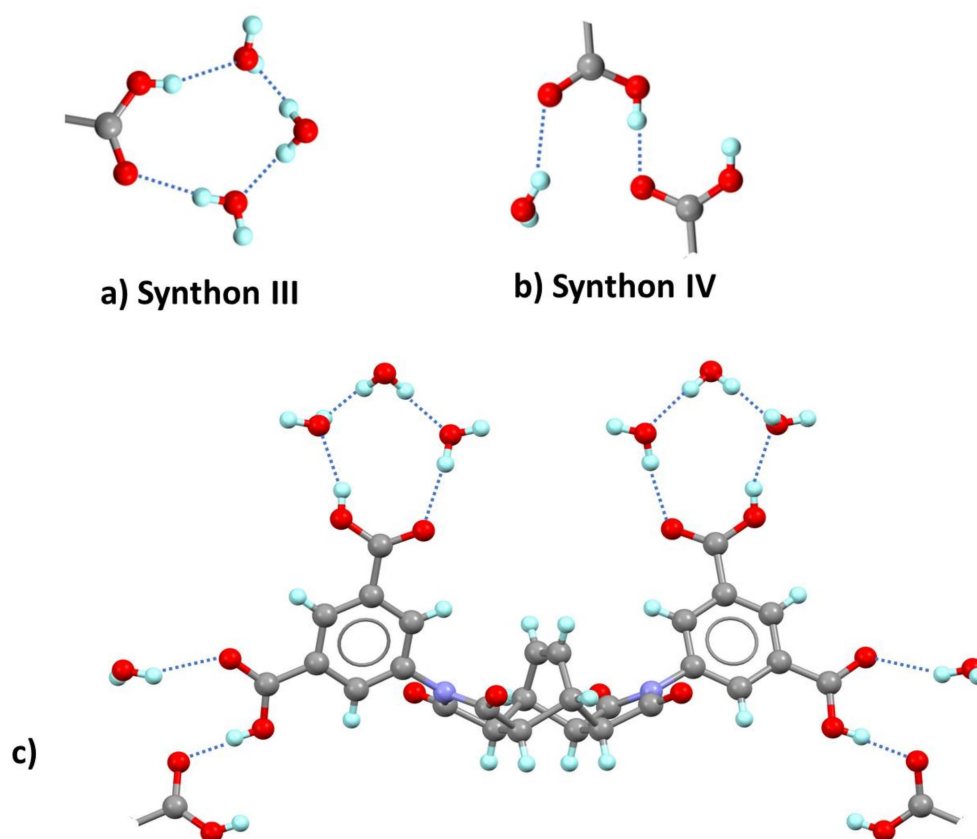


Figure 3. Two kinds of heterosynthons (a,b) and the H-bonds environment of one H_4PTTA (c) in **1-H**.

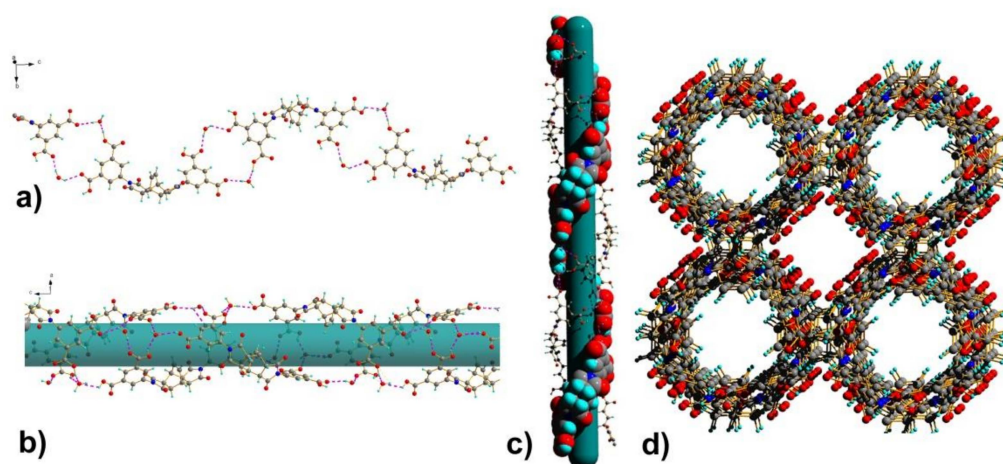
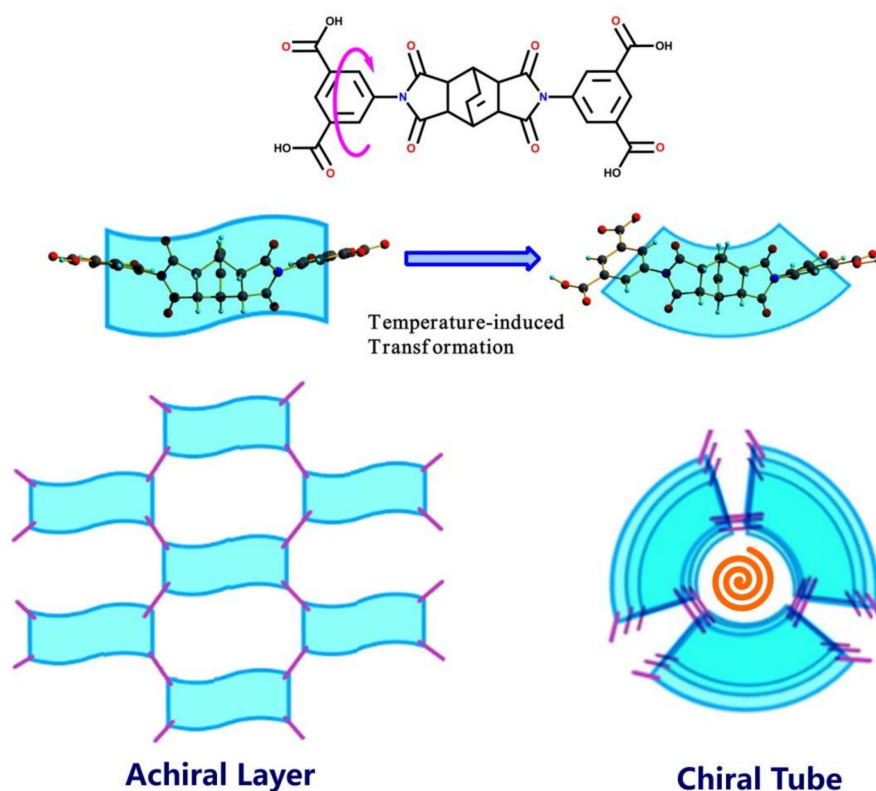


Figure 4. The mono-helix H-bond chain layer (a); the bi-helix chains interacted chiral H-bond tube (b,c); the packing of the hydrogen bonded tubes (d) in **1-H**.

3.3. Syntheses and Structural Comparison

Two isomeric supramolecular nets, **1-L** and **1-H**, built by tetra-acid are synthesized from the same starting reactants under different temperatures. Owing to its semi-rigid rotation of the C–N bond, both phenyl rings of tetra-acid H_4TPPA adopt dissimilar orientations with the changed torsion angles from 51.84° in **1-L** to 65.70° in **1-H**. The temperature-induced configuration transformation of H_4TPPA indicates that the structural variation in the final isomeric formed by H-bond frameworks (Scheme 2) is influenced by the temperature applied during the synthesis. Thus, H-bonded wave-layer **1-L** is formed at the room

temperature while the chiral H-bonded tube-like structure **1-H** is constructed at 160 °C under hydrothermal conditions.



Scheme 2. The supramolecular isomeric transformation derived from the ip segments torsion of semi-rigid tetra-acid ligands.

3.4. CD Spectroscopy

Analysis of the crystal structure suggests that **1-H** is a chiral supramolecular organic framework [32], which entails the self-assembly of homo-chiral (right-helix) tubes derived from the achiral semi-rigid tetra-acids being assembled via different hydrogen bond motifs. It has been confirmed in a kinetic model that an achiral artificial assembly system could spontaneously produce chirality [33]. However, without inducing the chiral chemical reagents (as reactants or template), the coordinated or covalent enantiomers are commonly observed in the spontaneous resolution system [34–37]. Although **1-H** should contain two different enantiomer single crystals, unfortunately, the attempt to pick out and solve the left-helix structure of single-crystal X-ray crystallography failed. However, the circular dichroism (CD) measurement based on more than 50 randomly picked crystals from one-pot resulted in solid CD spectroscopy, showing that **1-H** explicitly exhibits Cotton effects at about $\lambda = 215$ and 255 nm, which confirms that the right- and left-helix enantiomers were spontaneously resolved during the course of the crystallization in the one-pot hydrothermal reaction, as shown in Figure 5. The results indicate that more research into the rational syntheses strategy is required in order to figure out how to control the preparation of the homo-chiral H-bonded frameworks from spontaneous resolution.

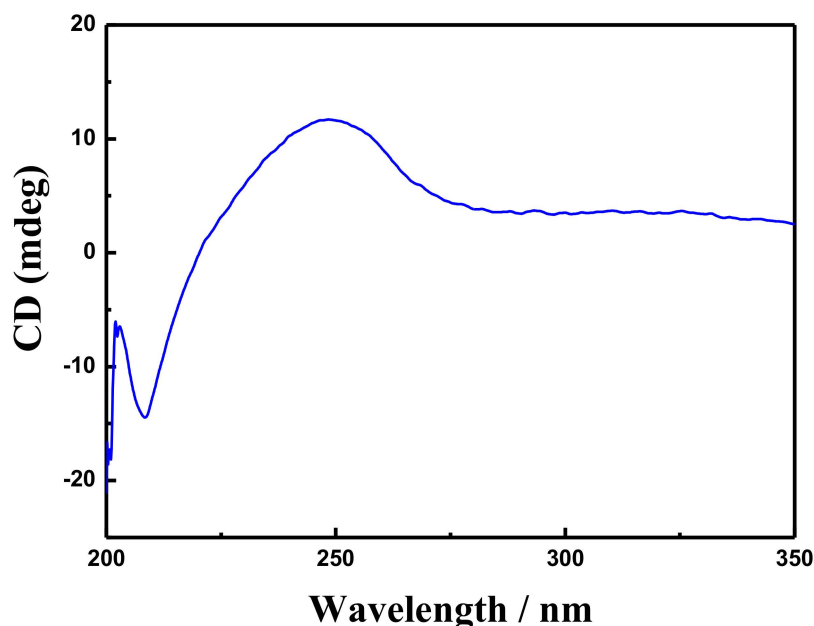


Figure 5. The solid-state circular dichroism (CD) spectra of stochastic of conglomerate **1-H**.

4. Conclusions

In this work, we have successfully synthesized two supramolecular compounds, namely **1-L** and **1-H**, starting from the same precursors, the mixture of semi-rigid tetra-acid H_4TPPA , H_2O and DMF. It is interesting that both supramolecular compounds performed variable hydrogen bond isomers under different synthesis temperatures. The room temperature approach leads to the formation of **1-L**, which features the H-bond layer structure based on the general dimeric homosynthon and one H_2O inserted dimmeric heterosynthon. **1-H** synthesized at $160\text{ }^\circ\text{C}$ under hydrothermal conditions, and results in the chiral H-bonded tube were based on two kinds of H-bond heterosynthons. Notably, the structural differences between two supramolecular isomers of **1-L** and **1-H** were derived from the rotation of the C-N bond of semi-rigid tetra-acid H_4TPPA , which induced the different torsion of both isophthalic acid segments within H_4TPPA .

Author Contributions: Conceptualization, J.Z., Y.-Y.L. and X.-F.W.; methodology, C.L. and X.-F.W.; software, C.T., Y.-Y.L. and X.-F.W.; validation, C.T. and X.-F.W.; formal analysis, Y.-Y.L. and X.-F.W.; investigation, J.Z., Y.-Y.L. and X.-F.W.; resources, X.-F.W.; data curation, C.L., C.T. and J.Z.; writing—original draft preparation, Y.-Y.L. and X.-F.W.; writing—review and editing, Y.-Y.L. and X.-F.W.; visualization, X.-F.W.; supervision, X.-F.W.; project administration, X.-F.W.; funding acquisition, J.Z., C.T. and X.-F.W. All authors have read and agreed to the published version of the manuscript.

Funding: This research was supported by Hunan Provincial Natural Science Foundation of China (grant number 2021JJ30565, 2020JJ5473 and 2019JJ50524), We wish to thank the financial support from University of South China (No. 2015XQD53).

Institutional Review Board Statement: Not applicable.

Informed Consent Statement: Not applicable.

Data Availability Statement: Crystallographic data for (**1-L** and **1-H**) have been deposited with the Cambridge Crystallographic Data Center as supplemental publication numbers CCDC No. 2118337 and 2118346, respectively. Copies of the data can be obtained free of charge via http://www.ccdc.cam.ac.uk/data_request/cif, (accessed on 11 September 2021), or by emailing data_request@ccdc.cam.ac.uk, or by contacting The Cambridge Crystallographic Data Centre, 12, Union Road, Cambridge CB2 1EZ, UK.

Conflicts of Interest: The authors declare no conflict of interest.

Sample Availability: Samples of the compounds are not available from the authors.

References

1. Pepinsky, R. Crystal engineering: New concept in crystallography. *Phys. Rev.* **1955**, *100*, 971.
2. Desiraju, G.R. *Crystal Engineering: The Design of Organic Solids*; Elsevier: Amsterdam, the Netherlands, 1989.
3. Desiraju, G.R. Crystal Engineering: A Holistic View. *Angew. Chem. Int. Ed.* **2007**, *46*, 8342–8356. [[CrossRef](#)] [[PubMed](#)]
4. Brammer, L. Developments in inorganic crystal engineering. *Chem. Soc. Rev.* **2004**, *33*, 476–489. [[CrossRef](#)] [[PubMed](#)]
5. Duggirala, N.K.; Perry, M.L.; Almarsson, Ö.; Zaworotko, M.J. Pharmaceutical cocrystals: Along the path to improved medicines. *Chem. Commun.* **2016**, *52*, 640–655. [[CrossRef](#)]
6. Yaghi, O.M.; O’Keeffe, M.; Ockwig, N.W.; Chae, H.K.; Eddaoudi, M.; Kim, J. Reticular Synthesis and the Design of New Materials. *Nature* **2003**, *423*, 705–714. [[CrossRef](#)]
7. Braga, D.; Brammer, L.; Champness, N.R. New trends in crystal engineering. *CrystEngComm* **2005**, *7*, 1–19. [[CrossRef](#)]
8. Hosseini, M.W. Molecular tectonics: From simple tectons to complex molecular networks. *Acc. Chem. Res.* **2005**, *38*, 313–323. [[CrossRef](#)]
9. Sasaki, T.; Sakamoto, S.; Takamizawa, S. Organoferroelastic Crystal Prepared by Supramolecular Synthesis. *Cryst. Growth Des.* **2020**, *20*, 1935–1939. [[CrossRef](#)]
10. Lin, R.B.; He, Y.; Li, P.; Wang, H.; Zhou, W.; Chen, B. Multifunctional Porous Hydrogen-Bonded Organic Framework Materials. *Chem. Soc. Rev.* **2019**, *48*, 1362–1389. [[CrossRef](#)]
11. Lehn, J.-M. From supramolecular chemistry towards constitutional dynamic chemistry and adaptive chemistry. *Chem. Soc. Rev.* **2007**, *36*, 151–160. [[CrossRef](#)]
12. Bis, J.A.; McLaughlin, O.L.; Vishweshwar, P.; Zaworotko, M.J. Supramolecular heterocatemers and their role in cocrystal design. *Cryst. Growth Des.* **2006**, *6*, 2648–2650. [[CrossRef](#)]
13. Aakeröy, C.B.; Beatty, A.M.; Helfrich, B.A. “Total synthesis” supramolecular style: Design and hydrogen-bond-directed assembly of ternary supermolecules. *Angew. Chem. Int. Ed.* **2001**, *40*, 3240–3242. [[CrossRef](#)]
14. Sokolov, A.N.; Friscic, T.; MacGillivray, L.R. Enforced face-to-face stacking of organic semiconductor building blocks within hydrogen-bonded molecular cocrystals. *J. Am. Chem. Soc.* **2006**, *128*, 2806–2807. [[CrossRef](#)] [[PubMed](#)]
15. Desiraju, G.R. Supramolecular synthons in crystal engineering—a new organic synthesis. *Angew. Chem. Int. Ed.* **1995**, *34*, 2311–2327. [[CrossRef](#)]
16. Joanna, A.B.; Vishweshwar, P.; Weyna, D.; Zaworotko, M.J. Hierarchy of supramolecular synthons: Persistent hydroxyl...pyridine hydrogen bonds in cocrystals that contain a cyano acceptor. *Mol. Pharm.* **2007**, *4*, 401–416.
17. Rajput, L.; Biradha, K. Design of cocrystals via new and robust supramolecular synthon between carboxylic acid and secondary amide: Honeycomb network with jailed aromatics. *Cryst. Growth Des.* **2009**, *9*, 40–42. [[CrossRef](#)]
18. Wang, L.; Xu, L.Y.; Xue, R.F.; Lu, X.F.; Chen, R.X.; Tao, X.T. Cocrystallization of N-donor type compounds with 5-sulfosalicylic acid: The effect of hydrogen-bonding supramolecular architectures. *Sci. China Chem.* **2012**, *55*, 138–144. [[CrossRef](#)]
19. Kanters, J.A.; Roelofsen, G. Hydrogen-Bond Motifs of Carboxylic Acids: The α -Form of Monochloroacetic Acid. *Acta Cryst. B* **1976**, *32*, 3328–3331. [[CrossRef](#)]
20. Kanters, J.A.; Roelofsen, G.; Feenstra, T. Hydrogen-Bond Motifs of Carboxylic Acids: The β -Form of Monochloroacetic Acid. *Acta Cryst. B* **1976**, *32*, 3331–3333. [[CrossRef](#)]
21. Leiserowitz, L. Molecular Packing Modes. Carboxylic Acids. *Acta Cryst. B* **1976**, *32*, 775–802. [[CrossRef](#)]
22. Rajput, L.; Jana, N.; Biradha, K. Carboxylic Acid and Phenolic Hydroxyl Interactions in the Crystal Structures of Co-Crystals/Clathrates of Trimesic Acid and Pyromellitic Acid with Phenolic Derivatives. *Cryst. Growth Des.* **2010**, *10*, 4565–4570. [[CrossRef](#)]
23. D’Ascenzo, L.; Auffinger, P. A comprehensive classification and nomenclature of carboxyl–carboxyl(ate) supramolecular motifs and related catemers: Implications for biomolecular systems. *Acta Cryst. B* **2015**, *71*, 164–175. [[CrossRef](#)]
24. Ou, G.; Wang, Q.; Zhou, Q.; Wang, X.-F. Phenol Derivatives as Co-Crystallized Templates to Modulate Trimesic-Acid-Based Hydrogen-Bonded Organic Molecular Frameworks. *Crystals* **2021**, *11*, 409. [[CrossRef](#)]
25. Wang, X.-F.; Zhang, Y.-B.; Xue, W.; Qi, X.-L.; Chen, X.-M. Two temperature-induced isomers of metal-carboxylate frameworks based on different linear trinuclear $\text{Co}_3(\text{RCOO})_8$ clusters exhibiting different magnetic behaviours. *CrystEngComm* **2010**, *12*, 3834–3839. [[CrossRef](#)]
26. Du, L.-Y.; Shi, W.-J.; Hou, L.; Wang, Y.-Y.; Shi, Q.-Z.; Zhu, Z. Solvent or Temperature Induced Diverse Coordination Polymers of Silver(I) Sulfate and Bipyrazole Systems: Syntheses, Crystal Structures, Luminescence, and Sorption Properties. *Inorg. Chem.* **2013**, *52*, 14018–14027. [[CrossRef](#)]
27. Moulton, B.; Zaworotko, M.J. From molecules to crystal engineering: Supramolecular isomerism and polymorphism in network solids. *Chem. Rev.* **2001**, *101*, 1629–1658. [[CrossRef](#)]
28. Bhattacharya, S.; Saha, B.K. Guest-induced isomerization of net and polymorphism in trimesic acid-arylamine complexes. *Cryst. Growth Des.* **2011**, *11*, 2194–2204. [[CrossRef](#)]
29. Wang, X.-F.; Chen, Y.; Song, L.-P.; Fang, Z.; Zhang, J.; Shi, F.; Lin, Y.-W.; Sun, Y.; Zhang, Y.-B.; Rocha, J. Cooperative Capture of Uranyl Ions by a Carbonyl-Bearing Hierarchical-Porous Cu–Organic Framework. *Angew. Chem. Int. Ed.* **2019**, *58*, 18808–18812. [[CrossRef](#)] [[PubMed](#)]
30. Sheldrick, G.M. Crystal structure refinement with SHELXL. *Acta Cryst. A* **2015**, *71*, 3–8. [[CrossRef](#)]
31. Spek, A.L.J. Single-crystal structure validation with the program PLATON. *Appl. Crystallogr.* **2003**, *36*, 7. [[CrossRef](#)]

32. Li, Y.; Li, Q.; Miao, X.; Qin, C.; Chu, D.; Cao, L. Adaptive Chirality of an Achiral Cucurbit[8]uril-Based Supramolecular Organic Framework for Chirality Induction in Water. *Angew. Chem. Int. Ed.* **2021**, *60*, 6744–6751. [[CrossRef](#)]
33. Frank, F.C. On spontaneous asymmetric synthesis. *Biochim. Biophys. Acta* **1953**, *11*, 459–463. [[CrossRef](#)]
34. Chen, Y.; Tan, C.; Song, L.-P.; Zhou, J.; Zeng, Q.; Xie, R.; Wang, X.-F. Two chiral cadmium carboxylate framework isomers generated by spontaneous resolution: Synthesis, structures and properties. *J. Coord. Chem.* **2019**, *72*, 251–261. [[CrossRef](#)]
35. Wu, D.; Zhou, K.; Tian, J.; Liu, C.; Tian, J.; Jiang, F.; Yuan, D.; Zhang, J.; Chen, Q.; Hong, M. Induction of Chirality in a Metal–Organic Framework Built from Achiral Precursors. *Angew. Chem. Int. Ed.* **2021**, *60*, 3087–3094. [[CrossRef](#)] [[PubMed](#)]
36. Roszak, K.; Katrusiak, A. High-pressure and temperature dependence of the spontaneous resolution of 1,1'-binaphthyl enantiomers. *Phys. Chem. Chem. Phys.* **2018**, *20*, 5305–5311. [[CrossRef](#)] [[PubMed](#)]
37. Kurdi, R.; Táborosi, A.; Zucchi, C.; Pályi, G. Autosolvation: Architecture and Selection of Chiral Conformers in Alkylcobalt Carbonyl Molecular Clocks. *Symmetry* **2014**, *6*, 551–565. [[CrossRef](#)]